Islamic Azad University
Mashhad Branch

Maleki and Madani / Iranian Journal of Earth Sciences 8 (2016) / 173-184

Multivariate geostatistical analysis: an application to ore body evaluation

Mohammad Maleki[1], Nasser Madani[*2]

1. Department of Mining Engineering, University of Chile, Santiago, Chile
2. Young Researchers and Elite Club, South Tehran Branch, Islamic Azad University, Tehran, Iran

Received 4 September 2015; accepted 17 April 2016

Abstract

It is now a common practice in the mining industry to deal with several correlated exploratory attributes, which need to be jointly simulated to reproduce their correlations and assess the multivariate grade risk. Approaches to multivariate simulation, which remove the correlation between attributes of interest prior to simulation and re-imposing of the relationship afterward, have been gaining popularity over the more common joint simulation methodologies. This is due to their better accuracy and computational efficiency as the number of attributes for simulation increases. Principal component analysis (PCA) is one of these approaches. However, PCA suffers from some drawbacks such as the factors that are uncorrelated just for collocated locations. Minimum/maximum autocorrelation factors (MAF) is a modification of the PCA method where the factors are uncorrelated for two lags. As an expectation, when the linear co-regionalization model contains only two nested structures, the factors do not have any spatial correlations. The main aim of this research is to compare the results of the MAF approach with some traditional approaches for multivariate simulation (co-simulation and independent simulation approaches). To this end, two variables have been simulated with three different methods and are then compared based on some yardsticks such as the ability to reproduce the original correlation coefficient between two variables. The results showed that MAF has the capability to reproduce the intrinsic correlation between the variables.

Keywords: *Geostatistical simulation, co-simulation, MAF, correlation*

1. Introduction

Geostatistical analysis has been widely used in the process of ore body evaluation. Simulation conveys an important part of uncertainty, which leads to quantifying risk in the mining and petroleum industry such as the grades of elements of interest, petrophysical properties of the subsoil, or geometallurgical properties (work index, acid consumption, metal recoveries) (Emery 2005; Emery et al. 2005; Emery and Lantuéjoul 2006; Ortiz 2006; Emery 2007; Chiles and Delfiner 2009; Emery and Robles 2009; Emery 2012; Montoya et al. 2012; Boisvert et al. 2013; Maleki-Tehrani et al. 2013; Rossi and Deutsch 2013). The practical implementation of geostatistical modelling requires specifying a stochastic model, which describes the spatial distribution of the exploratory co-regionalized variables (what should be simulated) and an algorithm, which aims at constructing realizations of the prescribed model (how it should be simulated: Chiles and Delfiner (2009); Lantuéjoul (2013)). Independent simulation in multi-element deposits does not consider the intrinsic correlation coefficient between the variables. Instead, co-simulation appreciates this parameter by calculating the cross-variograms.

---

*Corresponding author.
E-mail address (es): naser.madani@yahoo.com

Maximum/minimum autocorrelation factor (MAF) analysis (Switzer and Green 1984; Desbarats and Dimitrakopoulos 2000; Boucher and Dimitrakopoulos 2009; Lopes et al. 2011) is a factor-based approach that considers the uncorrelated factors to independently simulate and acknowledge the correlation coefficient internally (Desbarats and Dimitrakopoulos 2000). For a two-structure linear model of co-regionalization, the approach has the attractive feature of producing orthogonal factors ranked in the order of increasing spatial correlation.

The purpose of this paper is to assess the performance and check the accuracy of three methods of simulation (independent simulation, co-simulation, and MAF) in the multi-element deposits when there is a significant correlation between the exploratory variables, through actual case studies located in Rio Blanco-Los Bronces copper deposits in Chile.

2. Simulation methodologies

2.1. Independent simulation and co-simulation

An independent simulation of the random variables Z(x) is simply a realization of Z(x), randomly selected from the set of all possible realizations. Its construction requires the knowledge of the spatial continuity of this random variable characterized by direct-variograms at

the most minimum simplicity (Chiles and Delfiner 2009; Lantuéjoul 2013).
However, it is often interesting to construct numerical models that reproduce the joint distribution of several co-regionalized variables at unsampled locations, conditionally to the information available at sampling locations (conditional co-simulation). Because the variables are usually spatially cross-correlated, it is not sufficient to simulate each variable separately. Instead, a multivariate approach can be used and one needs to calculate the cross-variograms associated with direct-variograms for each variable (Emery 2008; Paravarzar et al. 2015).
However, in multivariate geostatistics such as co-simulation, a crucial and frequent problem is finding a model of the co-regionalization matrix that fits adequately in the mathematical sense to the empirical cross-variogram matrix (Goulard and Voltz 1992).

2.2. Minimum/maximum autocorrelation factors (MAF)

MAF is another methodology in the substitution for co-simulation that is a principal component-based approach (in fact, it is a modification of PCA). It transforms the original variables into factors, uncorrelated at any lag distance (Chiles and Delfiner 2009). In fact, MAF is mainly based on two successive spectral decompositions. The MAF factors are ranked in order of increasing spatial correlation. There are two ways to obtain the factors:
Model-based MAF Approach: This requires the direct and cross-spatial continuity of input data to be modelled by using a specific linear model of co-regionalization in order to derive the uncorrelated factors. Data-driven MAF approach: This method does not require a linear model of co-regionalization to obtain the corresponding factors.
With respect to the first approach (model-based MAF approach), one should follow the steps below:
In the first step, the original data should be transformed into the normal standard Gaussian data. Then, by using the linear model of co-regionalization (LMC), we should model the direct and cross variogram of transformed data:

$$\Gamma_Z(h) = B_1\gamma_1(h) + (B - B_1)\gamma_2(h) \quad (1)$$

where B is a correlation matrix between transformed data and $\gamma_2(h)$: variogram
Then, one should perform spectral decomposition of the variance-covariance matrix of $B = Q^T \Lambda Q$ and the obtaining matrixes of Q and Λ.

$$B = Q\Lambda Q^T \quad (2)$$

The multiplication by $\Lambda^{-1/2}$ and the multi-Gaussian assumption ensures that all derived factors have a standard normal distribution.

$$A = \Lambda^{-1/2} Q \quad (3)$$

The PCA factors are then defined as:

$$Y_{PCA} = A\,Z(u) = \Lambda^{-1/2} Q\,Z(u) \quad (4)$$

To calculate the MAF factors, one should derive the second rotation matrix. The matrix of B_1 will be obtained from the LMC fitted model. So, the matrix Q_1 and Λ_1 could be obtained easily:

$$\begin{cases} V = AB_1A^T \\ V = Q_1\Lambda_1Q_1^T \end{cases} \quad (5)$$

$$F_{MAF} = Q_1 Y_{PCA}$$
$$F_{MAF} = Q_1\Lambda^{-1/2} Q\,Z(u)$$
$$F_{MAF} = M\,Z(u)$$

M is the matrix for transforming the input data into factor.
With respect to the second approach (data-driven MAF approach), the only difference is that matrix Q_1 will be obtained by the decomposition of matrix $\Gamma_{PCA}(h)$ (variogram matrix of principle component). In fact, the eigenvectors of matrix $\Gamma_{PCA}(h)$ are equal to the eigenvectors of matrix V. Therefore, since $\Gamma_{PCA}(h)$ can be computed using only the input data, there is no need to fit the LMC. Note that the eigenvectors of $\Gamma_{PCA}(\Delta)$ depend on the separation distance and its selection is a delicate task (Chiles and Delfiner 2009; Wackernagel 2013).

3. Geological Setting

The Los Bronces-Rio Blanco deposit is located on the west side of the Andes in Central Chile about 70 km from Santiago in Chile (Fig. 1). Los Bronces is a breccia complex superimposed on the west side of an earlier major porphyry copper system (Warnaars et al. 1985). The Rio Blanco mine is currently exploiting the north-central part of this porphyry deposit and has started operating a large copper-bearing tourmaline breccia, Sur-Sur, about 2km south of the present mine. The Los Bronces-Rio Blanco deposit was formed on the east side of the San Francisco batholith. This intrusion is strongly peraluminous and has a calc-alkaline composition with an alkali-calcic affinity. The batholith took a minimum of 11.5m.y. to form from the early Miocene (20.1m.y.) to the late Miocene (8.6m.y.). The porphyry copper mineralization, alteration, and copper tourmaline breccias were formed over a period of at least 2.5m.y. between 7.4 and 4.9m.y. ago. A post-mineral volcanic neck or diatreme at La Copa had erupted within, and removed a large segment of the northern part of the porphyry copper system, thus marking the last evidence of magmatic activity in the area. K-Ar age determinations of biotites indicate the diatreme erupted in the early Pliocene between 4.9 and 3.9m.y. ago. The pre-breccia porphyry system exhibits propylitic, sericitic, silicic, and potassic alterations. A unique alteration feature of this system is the replacement of mafic minerals by specularitc and/or tourmaline within the propylitic zone. The porphyry system contains disseminated and stockwork copper-iron-molybdenum sulphide mineralization within an area of about 12km^2.

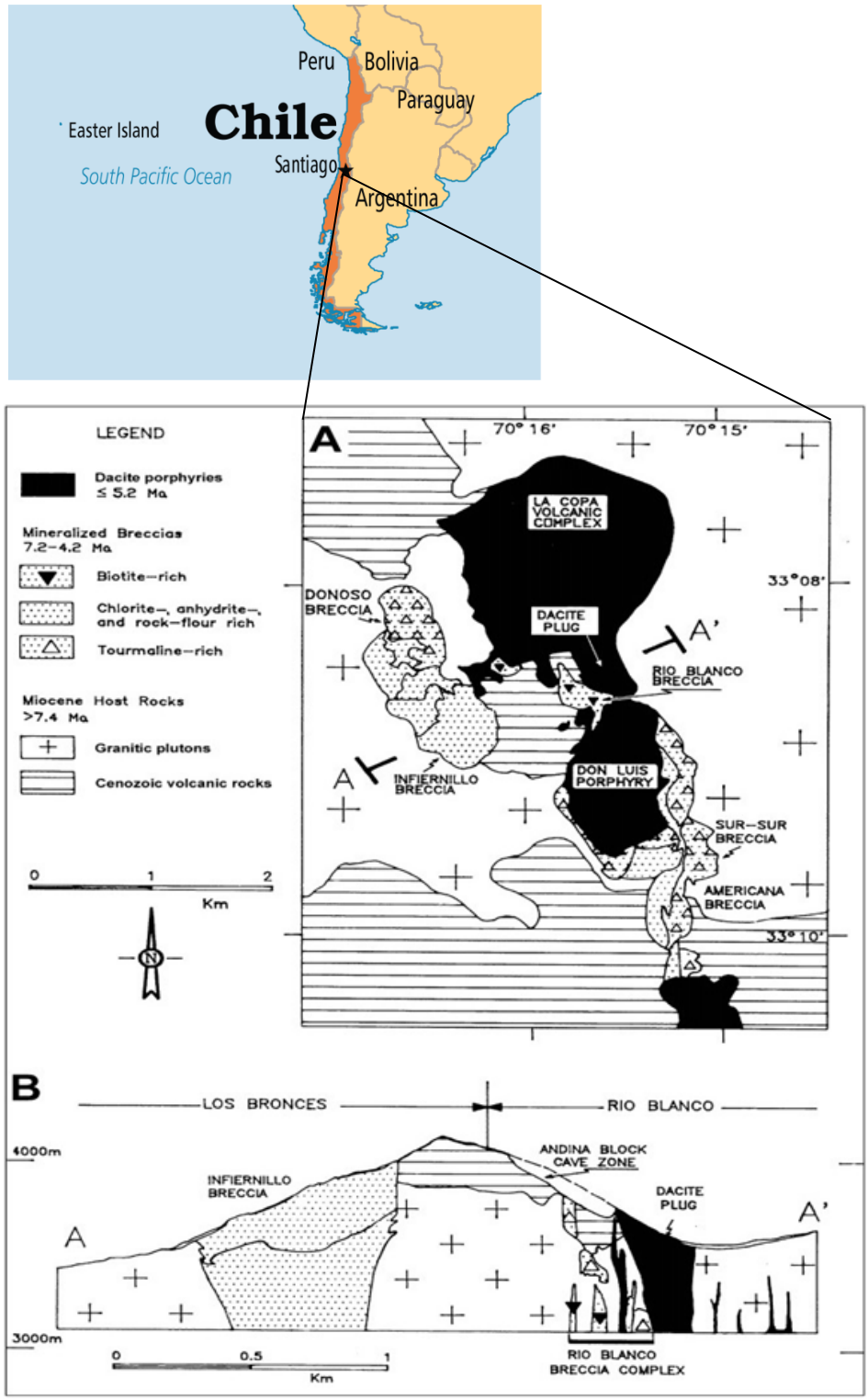

Fig. 1: Schematic map and a cross-section of the Rio Blanco-Los Bronces ore deposits (Warnaars et al. 1985)

Los Bronces is composed of at least seven different copper-bearing tourmaline breccias that form one large contiguous kidney-shaped body about 2km long and 0.7km wide, at the present erosion surface. The breccia body crops out at elevations between 4,150m and 3,450m. The various breccias are characterized by their locations, matrices, clasts, shapes, types, and degrees of mineralization and alteration. The breccias are usually monolithic, but in some cases are bilithic or heterolithic with most clasts consisting of quartz monzonite or andesite with locally minor amounts of quartz latite porphyry, monzodiorite, and vein quartz

(Warnaars et al. 1985). The breccia matrices consist of variable amounts of quartz, tourmaline, specularit, anhydrite, pyrite, chalcopyrite, bornite, molybdenite, sericite, chlorite, and rock flour. The seven different breccia types are identified from the oldest to the youngest as Ghost, Central, Western Infiernillo, Anhydrite, Fine Gray, and Donoso. The breccia complex has sharp contacts with the surrounding intrusive rocks and andesites. Internally, the breccia contacts are locally well-defined, but elsewhere they coalesce, inter-finger or display gradational contacts. The breccias at Los Bronces are interpreted as being emplaced explosively, followed by the collapse after pressure release of hydrothermal fluids. The primary mineral distribution is best known in the Donoso breccias, which has been the centre of mining activity since its discovery in 1864. In spite of the coarse and irregular nature of the sulphides in the matrix, chalcopyrite, pyrite, and specularit at the 3,670-m, open-pit operating level show a tendency to be distributed in irregular shells in which one of the three minerals predominates in any one shell. The transitions between shells are rapid. Several semi-ellipsoidal shells of alternating high and low copper grades are also apparent from the copper distribution of underground level 3640m and from various cross sections. The shells are approximately vertical and sub-parallel to the Donoso breccia contacts, which dip inward. Secondary enrichment enhanced the primary grade in the southern two-thirds of the Los Bronces breccia complex and in much of the surrounding porphyry copper systems. The degree and depth of enrichment are the functions of breccia and fracture permeability, and it extends to a depth of more than 500m in certain favourable sectors. The shape and depth of the enrichment blanket and overlying leached capping suggest that the enrichment process is related to the present ground-water regime and is still active (Warnaars et al. 1985).

4. Exploratory Data Analysis

The data for the analysis were gathered from 9,999 exploratory boreholes through the Rio Blanco-Los Bronces copper deposits. They were then composited to 3m in order to homogenize the support of the original data used in the process of geostatistical modelling. This procedure also reduces the variability of the dataset (Rossi and Deutsch, 2014). The area covered is about 2,822,791.5m^2 by drill holes conveying an acceptable distribution for sampling all parts over the deposit (Fig. 2). Exploratory data analysis was done through the composited dataset for two elements (SiO_2 and Cr) and the statistical parameters of this available data are presented in Table (1). Here, they are necessary beyond any decision-making.

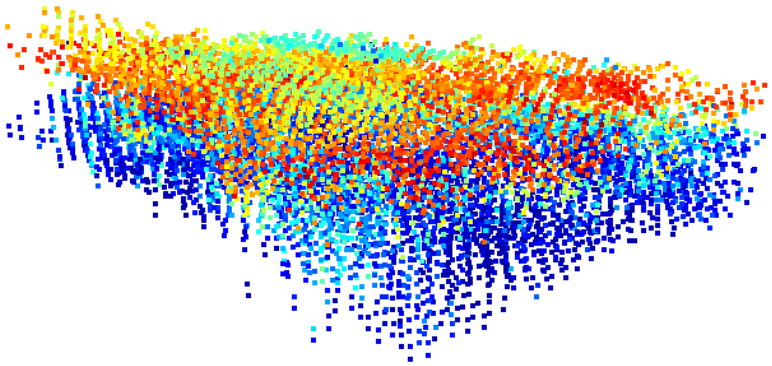

Fig. 2: 3D view of boreholes dataset; blue represents the low-grade areas and red the high grade areas; the grades are increasing from blue to red.

The goal of this research is to compare the conventional method of simulation and co-simulation with the new methodology entitled MAF. Therefore, an important key parameter for this examination is considering the correlation coefficient between these two variables (Chiles and Delfiner 2009). This coefficient summarizes the linear relationship (proportionality relationship) between two variables SiO_2 and Cr through a value between -1 and 1. This coefficient is -83.51% and one can conclude that there is a considerable relationship between these two variables.

The scatter plot is also helpful in intuitively determining the dependence relationship between two variables and detecting possible anomalous data. As can be seen from Figure 3, this negative relationship is strong as enough to implement the co-simulation.

Table 1: Statistical parameters for two underlying variables; these parameters are calculated through the sampling points.

Statistics	Min	Max	Mean
Cr	0.18%	4.46%	1.5%
SiO_2	2.1%	78.51%	28.94%

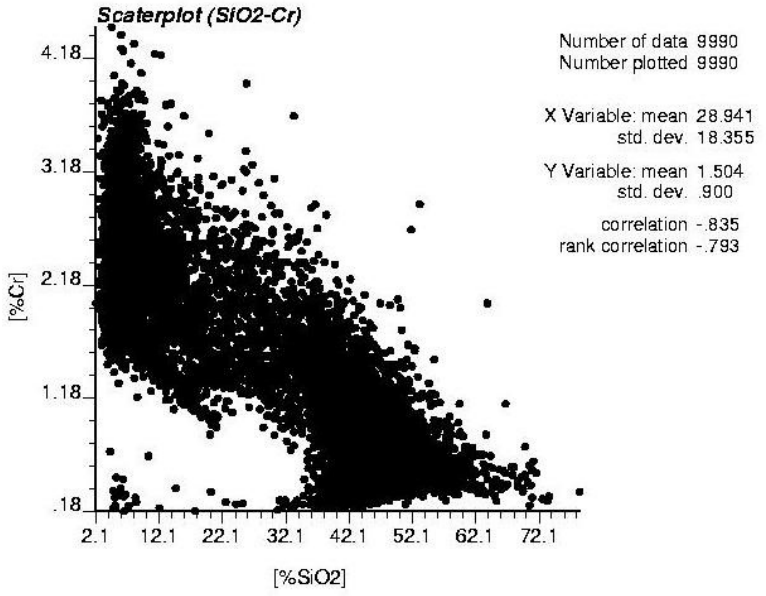

Fig. 3: Scatter plot between two variables SiO_2 and Cr

5. Variogram Analysis

Spatial continuity for implementing the co-simulation should be characterized by the cross-variogram associated with analysing the direct-variograms for the variables, respectively. The cross-variogram was first introduced by Matheron (1965) as the natural generalization of the variogram (Chiles and Delfiner 2009). This experimental cross-variogram matrix then should be modelled as a trial-error methodology. This theoretical model is entitled 'Linear Co-regionalization Model (LCM)' and it is applicable to any multivariate spatial data analysis (Golard and Voltz, 1992; Wakernagell, 2014). It is worth mentioning that these instructions require the data to be normally distributed and declustered (Chiles and Delfiner 2009). The declustering technique has been done prior to any analysis to allow us to assign each datum a weight based on the closeness to the surrounding data for alleviating the high-pseudo frequency occurring in high-graded areas. The declustered data is then transformed to the standard normal distribution.

Direct and cross-variogram for SiO_2 and Cr are depicted in Figure 4. The theoretical models of LCM are also fitted to the experimental ones as provided by Table 2.

6. Simulation and co-simulation

In this step, two variables of SiO_2 and Cr are modelled via two methodologies. The first considers the independent simulation for each variable and the second one acknowledges the correlation coefficient between two variables by co-simulation. As mentioned above, both variables are transformed to the Gaussian space with mean 0 and variance 1 (N(0,1)) and the variogram analysis has been done over the normal standard data. Note that for independent simulation, one just needs to apply the direct-variograms of SiO_2 and Cr, while the co-simulations deal with the cross-variogram as well as the direct ones. The simulation methodology in this study is turning the band (Emery and Lanteljoul 2006), in which it prioritizes other approximate approaches of simulation (Paravarzar et al. 2015). The most important parameters of simulations are provided as below:

Block Properties:

Volume in 3D: 2 408 540 m^3

Dimension in the east direction: 1.5m; Number of blocks in the east direction: 125

Dimension in the north direction: 1.5m; Number of blocks in the east direction: 138
Dimension in the elevation direction: 2m; Number of blocks in the east direction: 38
So, the total number of blocks is 655,500 through the region.
Number of realizations: 100
Seed for random number generation: 98457638
Dividing data into octant with three pieces of data per octant.
Kriging type; independent simulation: Simple kriging & Co-simulation: Co-kriging
Number of lines in turning band simulation: 1,000

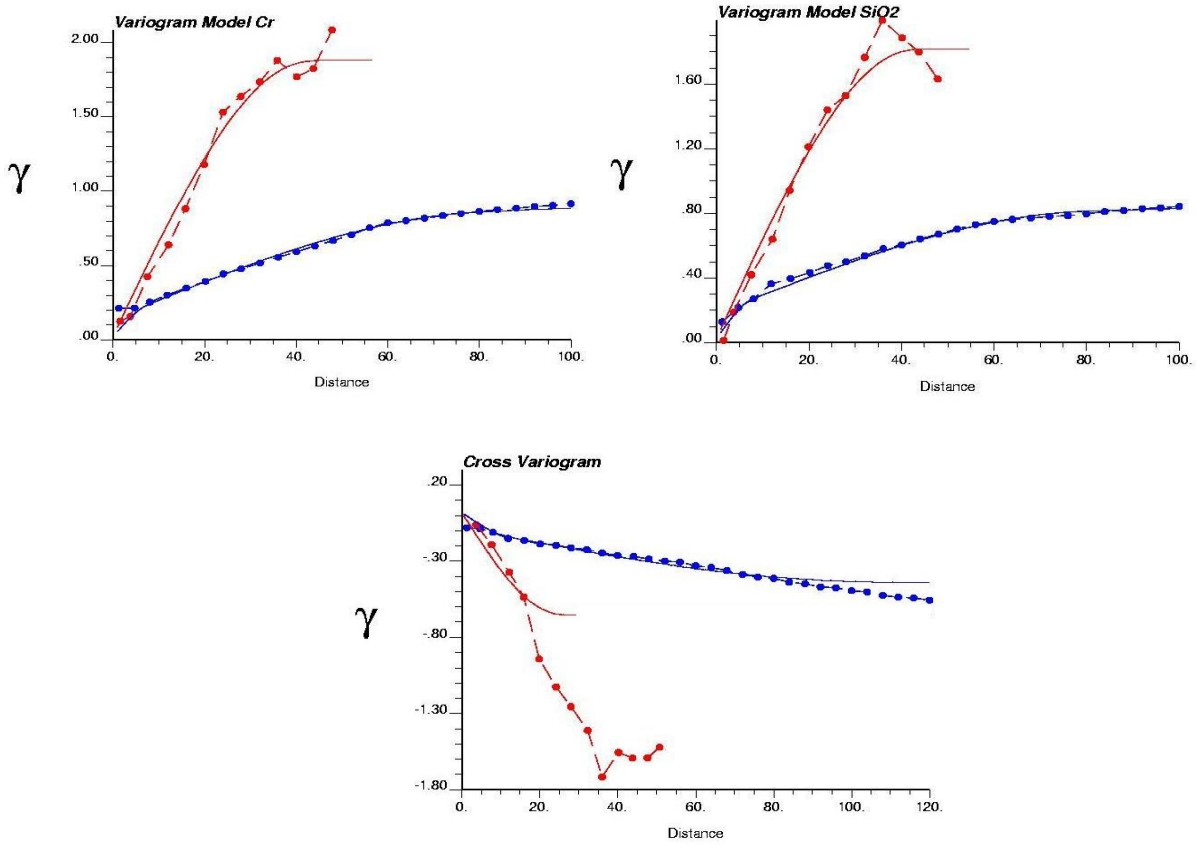

Fig. 4: Experimental and theoretical variogram and cross variogram of normal score data; blue: horizontal; red: vertical

Table 2: Properties of variogram model

Variogram model of Cr	Variogram model of SiO_2	Cross-variogram model
0.02 nugget	0.02 nugget	0.02 nugget
+0.12 Sph (12,12,20)	+0.16 Sph (12,12,20)	+(−0.1) Sph (12,12,20)
+0.53 sph (95,95,25)	+0.515 sph (95,95,25)	+(−0.15) sph (95,95,25)
+0.21Sph(120,120,27)	+0.125Sph(120,120,27)	+(−0.21)Sph(120,120,27)
+0.24Sph(inf, inf, 27)	+0.19Sph(inf, inf, 27)	+(−0.213)Sph(inf, inf, 27)

Co-regionalization model formulae:

$$\begin{pmatrix} \gamma_{sio2} & \gamma_{sio2-cr} \\ \gamma_{sio2-cr} & \gamma_{cr} \end{pmatrix} \quad (6)$$

$$\begin{pmatrix} 0.02 & 0.02 \\ 0.02 & 0.02 \end{pmatrix} \text{nugget} + \begin{pmatrix} 0.16 & -0.1 \\ -0.1 & 0.12 \end{pmatrix} \text{sph}(12,12,20) + \begin{pmatrix} 0.515 & -0.15 \\ -0.15 & 0.53 \end{pmatrix} \text{sph}(95,95,25) + \begin{pmatrix} 0.125 & -0.21 \\ -0.21 & 0.21 \end{pmatrix} \text{sph}(120,120,27) + \begin{pmatrix} 0.19 & -0.213 \\ -0.213 & 0.24 \end{pmatrix} \text{sph}(\text{inf}, \text{inf}, 27)$$

6.1. Comparison between independent simulation and co-simulation

In order to make a comparison, one can examine the statistical parameters of the produced realizations to see to what extent they are close to or far from the statistical parameters of the original row data. The following graphs (Figs. 5 and 6) show the box plot of the mean and variance of realizations for two variables (Cr and SiO_2), which were obtained from two different approaches (simulation and co-simulation). In terms of the mean, the obtained mean for both variables from the simulation and the co-simulation method is not very close to the mean of the raw data. However, the obtained variances from simulation and co-simulation for both variables are approximately close to the variance of raw data. Generally, with respect to the obtained mean and variance from these two approaches, there is no substantial difference between co-simulation and simulation, and one can just see subtle differences between these two methods.

In contrast to the mean and variance, there is a significant difference between simulation and co-simulation if one considers the correlation coefficient as a yardstick for comparing these two approaches. The reproduced correlation coefficient (Table. 3), which is obtained from simulation, is very far from the correlation coefficient of raw data (-0.8351). However, the co-simulation approach can reproduce the dependency between two variables better than independent simulations and the obtained correlation coefficient with the co-simulation method is somehow close to the correlation coefficient of raw data. So far, we have had some criteria for comparing the current simulation approaches (independent simulation, and co-simulation). In terms of reproducing variance and mean, we saw that there is no significant difference between independent simulation and co-simulation. However, if one considers the correlation coefficient as a yardstick, there is a substantial difference between these two approaches and one can say that the co-simulation is more capable of reproducing the dependency of two variables.

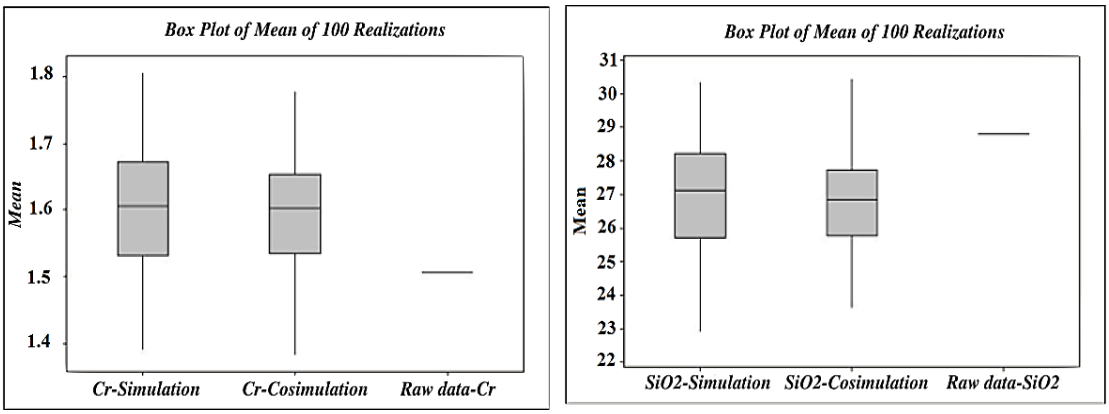

Fig 5. Box plot of mean of 100 realizations

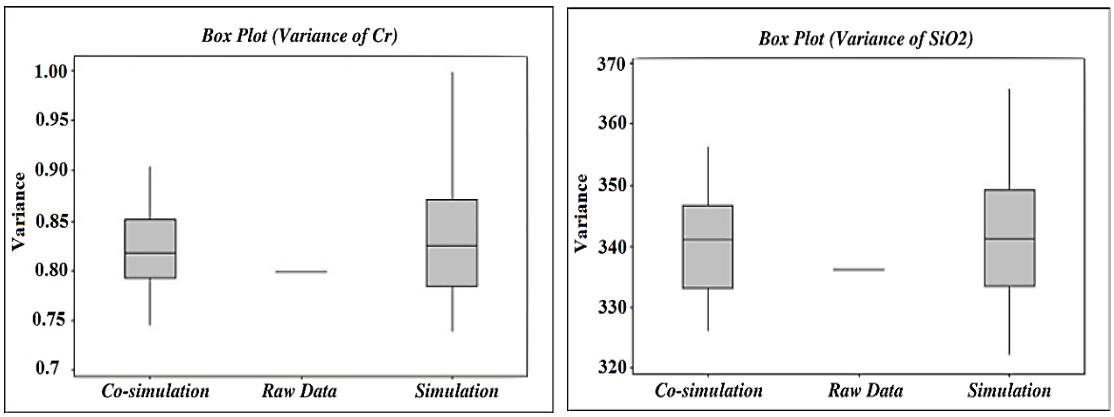

Fig 6. Box plot of variance of 100 realizations

Table 3: Correlation coefficient between Cr and SiO_2 in some realizations for two different methods through just 100 realizations.

	Simulation	Co-simulation
No.10	-0.04	-0.68194
No.11	0.011	-0.63628
No.12	0.057	-0.66218
No.13	-0.06	-0.69872
No.14	-0.063	-0.64814
No.15	0.003	-0.61169
No.16	-0.031	-0.68712
No.17	0.052	-0.66861
No.18	-0.028	-0.66363
No.19	-0.078	-0.67638

7. MAF method for simulation of variables

In order to obtain uncorrelated factors at any lags, we have to use just two nested structures (Wakernagel, 2014). So, we need to perform variogram analysis again for deriving the theoretical models with two nested structures.

Co-regionalization model with two nested structures (Chiles and Delfiner, 2009):

$$\begin{pmatrix} \gamma_{sio2} & \gamma_{sio2-cr} \\ \gamma_{sio2-cr} & \gamma_{cr} \end{pmatrix} \quad (7)$$
$$+\begin{pmatrix} 0.87 & -0.53 \\ -0.53 & 0.8 \end{pmatrix} \mathrm{sph}(120,120,20)$$
$$+\begin{pmatrix} 0.13 & -0.1428 \\ -0.1428 & 0.2 \end{pmatrix} \mathrm{sph}(\inf,\inf,30)$$

To obtain the factors, we need two transformation matrices (PCA and MAF transformation matrix):

$$\mathrm{PCA} = \begin{bmatrix} -0.5467 & 0.5467 \\ -1.2361 & -1.2361 \end{bmatrix}$$

$$\mathrm{MAF} = \begin{bmatrix} 0.0277 & -0.9811 \\ 1.3514 & 0.9297 \end{bmatrix}$$

As mentioned earlier, the obtained factors should be uncorrelated. Matrix K shows the correlation coefficients between the factors.

$$\mathrm{K} = \begin{bmatrix} 1 & -4.79e-16 \\ -4.79e-16 & 1 \end{bmatrix}$$

Also, the obtained factor should have a standard Gaussian distribution. This table shows the histogram of obtained factors and, as can be seen, both the factors have standard Gaussian distribution (Fig. 7).

Fig 7. Histogram of MAF factors

As mentioned, in the MAF methodology, the factors should be uncorrelated for any lag. So, we calculated the cross correlogram between the factors in order to see whether the factors are uncorrelated. The table below shows the cross correlogram between two factors for different lag separation distances (Fig. 8).

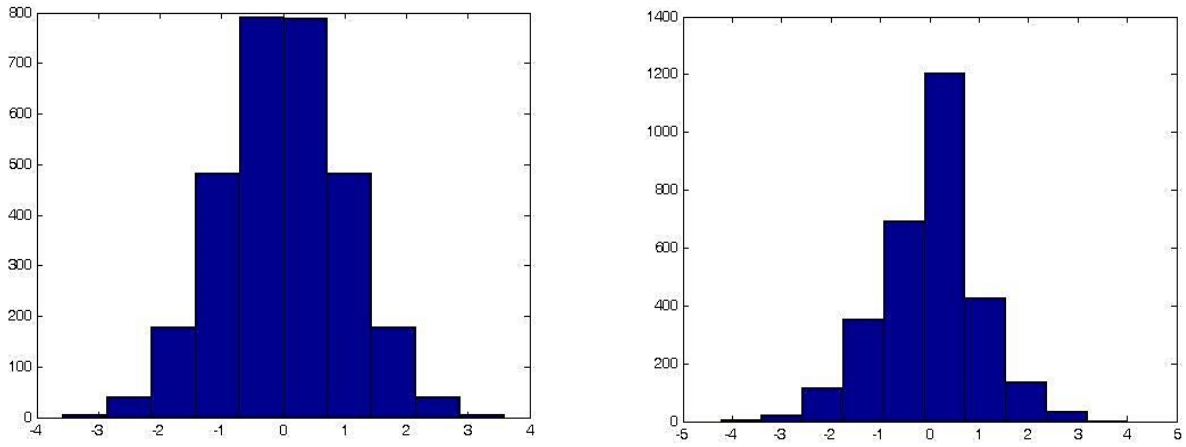

Fig 7. Histogram of MAF factors

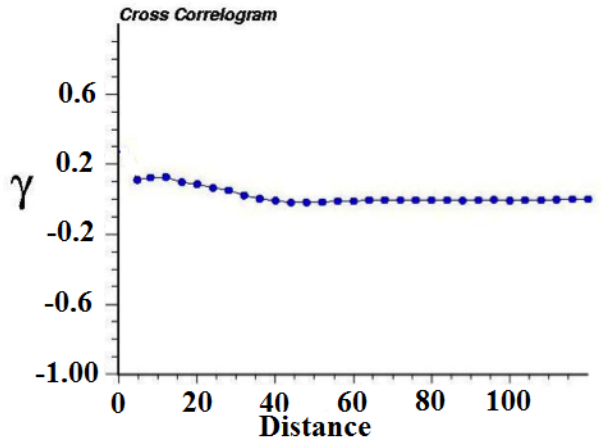

Cross correlogram for h=4m

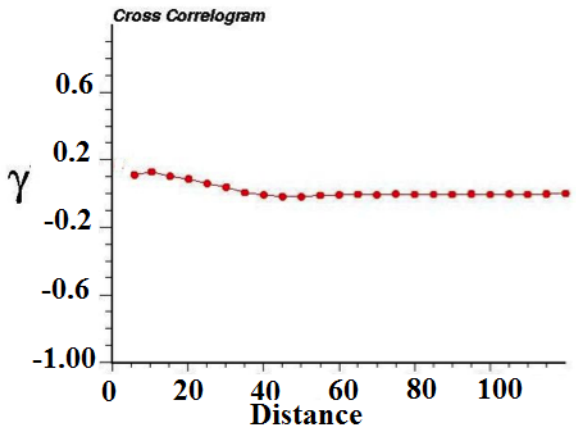

Cross correlogram for h=5m

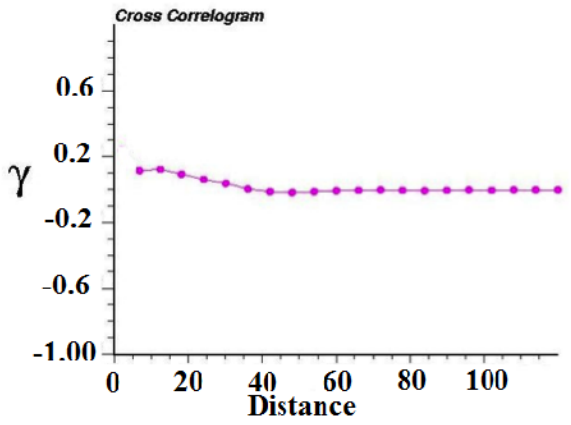

Cross correlogram for h=6m

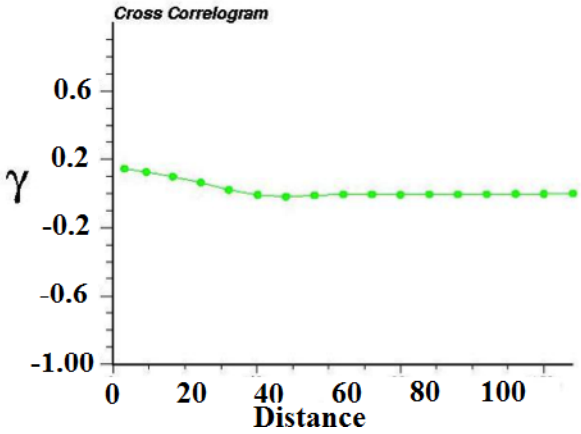

Cross correlogram for h=8m

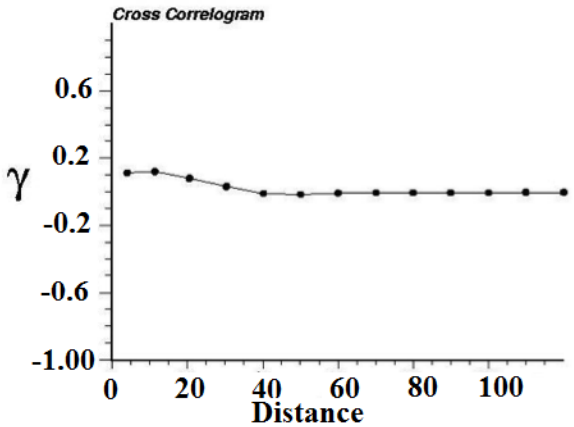

Cross correlogram for h=10m

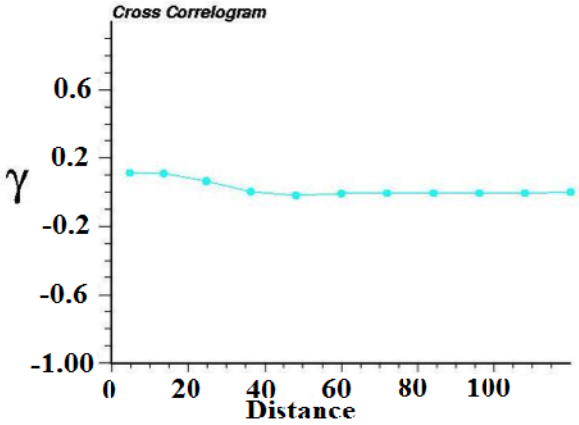

Cross correlogram for h=12m

Fig 8. Cross correlogram between two factors

7.1. Comparison between three methodologies

In this part, for making an intuitive comparison between the three approaches applied (i.e. independent simulation, co-simulation, and MAF), following the previous section, the box plot of variance and the mean of variables have been drawn for these three approaches. Closeness to the statistical parameters of raw data is a significant yardstick for this comparison. As depicted in Figures 9 and 10, it can be deduced that the variance and mean of variables, which is obtained from the MAF method, is closer to the variance of raw data in comparison to the other methods (simulation and co-simulation). After the MAF method, one can say that the results of the co-simulation method are closer to the original raw dataset.

Figure 10 shows the box plot of correlation coefficient as another important key factor to make a comparison, which is obtained from different methods (MAF, co-simulation and independent simulation). As can be seen from Figure 11, the obtained correlation coefficient from MAF is closer to the correlation coefficient of raw data. As expected, after the MAF approach, the obtained correlation coefficient from co-simulation is closer to the correlation coefficient of the raw data.

In Figure 12, it is worth showing the two section maps obtained from averaging between 100 realizations. Here, one can see the negative relationship as expected between the variables (Cr and SiO_2). In the high-graded area over the SiO_2, one can find the low-graded boundary in the Cr map. So, it can be an interesting result for reproducing the underlying correlation coefficient in the MAF methodology.

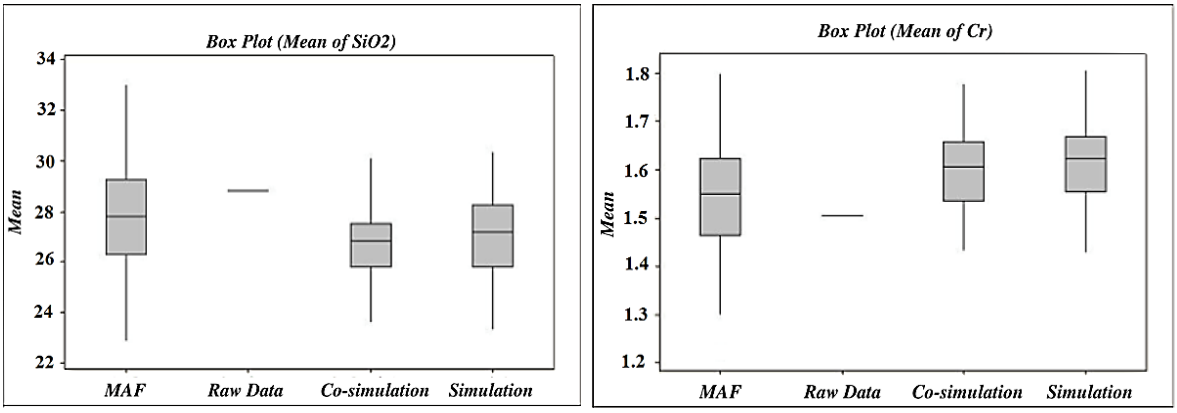

Fig 9. Mean of SiO_2 and Cr using different methods

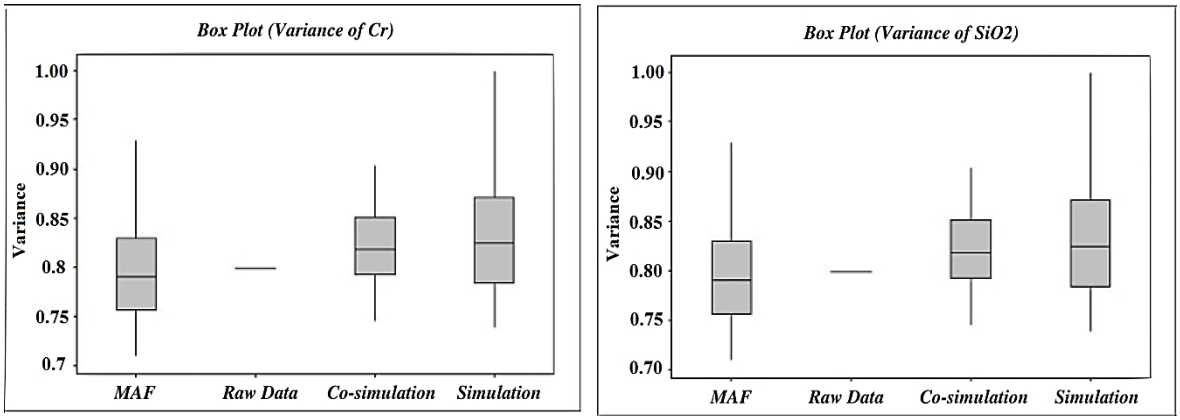

Fig 10. Variance of SiO_2 and Cr using different methods

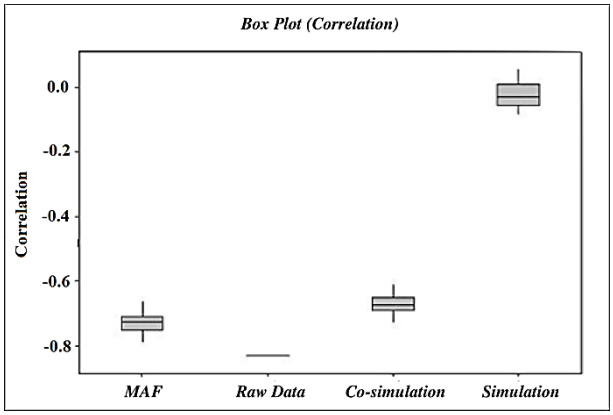

Fig 11. Obtained correlation using different methods

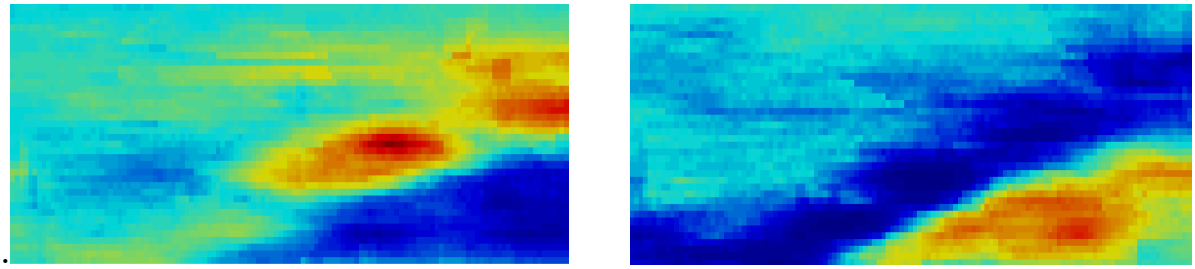

Cr- MAF (obtained from 100 realizations) SiO_2- MAF (obtained from 100 realizations)

Fig. 12: Map of Cr and SiO_2 obtained from MAF methodology; blue: low-grade area; red: high-grade area; from blue to red, the grades are in increasing order.

8. Conclusion

In this study, three different approaches of simulations (independent simulation, co-simulation, and MAF) are compared. One can choose different criteria and compare these three methods. By considering the correlation coefficient as a yardstick for comparing these three methods, we can see substantial differences between the three methods. Independent simulation of each variable could not reproduce the correlation coefficient between the variables (the obtained correlation is very far from the real correlation coefficient). The MAF method can reproduce the dependency of variables better than the co-simulation approach. However, the obtained correlation coefficient is not exactly identical with the correlation coefficient of raw data, but close to this and better than other methods.

Furthermore, in terms of variance and mean, there is no significant difference between these three methods. However, the obtained variance and mean of the MAF approach is closer to the variance and mean of the original data. Despite all advantages that are considered using the MAF method, it also has some drawbacks. The main drawback of the MAF approach is that this method only produces uncorrelated factors at any lag, if and only if we use the co-regionalization model with two nested structures. This is a huge restriction, especially when the data has a complex spatial continuity that can be modelled only with more than two nested structures.

References

Boisvert JB, Rossi ME, Ehrig K, Deutsch CV (2013) Geometallurgical modeling at Olympic dam mine, South Australia, *Mathematical Geosciences* 45:901-925.

Boucher A, Dimitrakopoulos R (2009) Block simulation of multiple correlated variables, *Mathematical Geosciences* 41:215-237.

Chiles J-P, Delfiner P (2009) Geostatistics: modeling spatial uncertainty vol 497. John Wiley & Sons.

Desbarats A, Dimitrakopoulos R (2000) Geostatistical simulation of regionalized pore-size distributions using min/max autocorrelation factors, *Mathematical Geology* 32:919-942.

Emery K (2007) Probabilistic modelling of lithological domains and it application to resource evaluation,

Journal of the Southern African Institute of Mining and Metallurgy 107:803-809.

Emery X (2005) Simple and ordinary multigaussian kriging for estimating recoverable reserves, *Mathematical Geology* 37:295-319.

Emery X (2008) A turning bands program for conditional co-simulation of cross-correlated Gaussian random fields, *Computers & Geosciences* 34:1850-1862.

Emery X (2012) Co-simulating total and soluble copper grades in an oxide ore deposit, *Mathematical Geosciences* 44:27-46.

Emery X, Bertini J, Ortiz J (2005) Resource and reserve evaluation in the presence of imprecise data, *CIM Bulletin* 98:2000.

Emery X, Lantuéjoul C (2006) Tbsim: A computer program for conditional simulation of three-dimensional gaussian random fields via the turning bands method, *Computers & Geosciences* 32:1615-1628.

Emery X, Robles LN (2009) Simulation of mineral grades with hard and soft conditioning data: application to a porphyry copper deposit, *Computational Geosciences* 13:79.

Goulard M, Voltz M (1992) Linear coregionalization model: tools for estimation and choice of cross-variogram matrix, *Mathematical Geology* 24:269-286

Lantuéjoul C (2013) Geostatistical simulation: models and algorithms. Springer Science & Business Media.

Lopes J, Rosas C, Fernandes J, Vanzela G (2011) Risk quantification in grade-tonnage curves and resource categorization in a lateritic nickel deposit using geologically constrained joint conditional simulation, *Journal of Mining Science* 47:166-176.

Maleki-Tehrani M, Asghari O, Emery X (2013) Simulation of mineral grades and classification of mineral resources by using hard and soft conditioning data: application to Sungun porphyry copper deposit, *Arabian Journal of Geosciences* 6:3773-3781.

Montoya C, Emery X, Rubio E, Wiertz J (2012) Multivariate resource modelling for assessing uncertainty in mine design and mine planning, *Journal of the Southern African Institute of Mining and Metallurgy* 112:353-363.

Ortiz X (2006) Geostatistical estimation of mineral resources with soft geological boundaries: a comparative study, *Journal of the Southern African Institute of Mining and Metallurgy* 106:577-584.

Paravarzar S, Emery X, Madani N (2015) Comparing sequential Gaussian and turning bands algorithms for cosimulating grades in multi-element deposits, *Comptes Rendus Geoscience* 347:84-93.

Rossi ME, Deutsch CV (2013) Mineral resource estimation. Springer Science & Business Media.

Switzer P, Green AA (1984) Min/max autocorrelation factors for multivariate spatial imagery, *Computer science and statistics*:13-16.

Wackernagel H (2013) Multivariate geostatistics: an introduction with applications. Springer Science & Business Media.

Warnaars FW, Holmgren C, Barassi S (1985) Porphyry copper and tourmaline breccias at Los Bronces-Rio Blanco, Chile, *Economic Geology* 80:1544-1565.